

RESEARCH ARTICLE

T-cell activation and bacterial infection in skin wounds of recessive dystrophic epidermolysis bullosa patients

Vitali Alexeev¹ | Leonie Huitema¹ | Taylor Phillips¹ | Rodrigo Cepeda^{2,3} |
Diego de los Cobos² | Regina Isabella Matus Perez² | Mauricio Salas-Garza² |
Oscar R. Fajardo-Ramirez⁴ | Franziska Ringpfeil⁵ | Jouni Uitto¹ |
Julio Cesar Salas-Alanis^{2,3} | Olga Igoucheva¹

¹Department of Dermatology and Cutaneous Biology, Sidney Kimmel Medical College, Thomas Jefferson University, Philadelphia, Pennsylvania, USA

²DEBRA MEXICO, Guadalupe, Mexico

³Julio Salas Dermatology, Guadalupe, Mexico

⁴School of Medicine and Health Sciences, Technological University of Monterrey, Monterrey, Mexico

⁵Ringpfeil Advanced Dermatology, Haverford, Pennsylvania, USA

Correspondence

Olga Igoucheva, Department of Dermatology and Cutaneous Biology, Sidney Kimmel Medical College, Thomas Jefferson University, 233 S. 10th Street, BLSB, Rm. 430, Philadelphia, PA 19107, USA.

Email: olga.igoucheva@jefferson.edu

Funding information

U.S. Department of Defense, Grant/Award Number: W81XWH1810628

Abstract

Recessive dystrophic epidermolysis bullosa (RDEB) patients develop poorly healing skin wounds that are frequently colonized with microbiota. Because T cells play an important role in clearing such pathogens, we aimed to define the status of adaptive T cell-mediated immunity in RDEB wounds. Using a non-invasive approach for sampling of wound-associated constituents, we evaluated microbial contaminants in cellular fraction and exudates obtained from RDEB wounds. Infectivity and intracellular trafficking of inactivated *Staphylococcus aureus* was assessed in RDEB keratinocytes. *S. aureus* and microbial antigen-specific activation of RDEB wound-derived T cells were investigated by fluorescence-activated cell sorting-based immune-phenotyping and T-cell functional assays. We found that RDEB wounds and epithelial cells are most frequently infected with *Staphylococcus* sp. and *Pseudomonas* sp. and that *S. aureus* essentially infects more RDEB keratinocytes and RDEB-derived squamous cell carcinoma cells than keratinocytes from healthy donors. The RDEB wound-associated T cells contain populations of CD4⁺ and CD8⁺ peripheral memory T cells that respond to soluble microbial antigens by proliferating and secreting interferon gamma (IFN γ). Moreover, CD8⁺ cytotoxic T lymphocytes recognize *S. aureus*-infected RDEB keratinocytes and respond by producing interleukin-2 (IL-2) and IFN γ and degranulating and cytotoxicity killing infected cells. Prolonged exposure of RDEB-derived T cells to microbial antigens in vitro does not trigger PD-1-mediated T-cell exhaustion but induces differentiation of the CD4^{high} population into CD4^{high}CD25⁺FoxP3⁺ regulatory T cells. Our data demonstrated that adaptive T cell-mediated immunity could clear infected cells from wound sites, but these effects might be inhibited by PD-1/Treg-mediated immuno-suppression in RDEB.

KEYWORDS

infection, RDEB, T-cell immunity, wound healing

This is an open access article under the terms of the [Creative Commons Attribution-NonCommercial-NoDerivs](https://creativecommons.org/licenses/by-nc-nd/4.0/) License, which permits use and distribution in any medium, provided the original work is properly cited, the use is non-commercial and no modifications or adaptations are made.

© 2022 The Authors. *Experimental Dermatology* published by John Wiley & Sons Ltd.

1 | INTRODUCTION

Recessive dystrophic epidermolysis bullosa (RDEB) is a hereditary mechanobullous disease caused by mutations in *COL7A1* gene that lead to a lack or dysfunction of type VII collagen (Col7), weak adhesion of skin layers and extreme fragility of the skin.¹ RDEB patients commonly develop skin lesions following minor mechanical stress to the skin and blisters that progress to poorly healing wounds, having a detrimental effect on quality of life. Human skin is home to a wide array of commensal microorganisms. Most common commensal species include *Staphylococcus* and *Micrococcus* bacteria, and *Malassezia* fungi.² These and many other commensals establish symbiotic relations with host immune system and prevent potentially harmful foreign bacteria from colonizing the skin. When skin integrity is compromised, wounds are frequently invaded by microorganisms that acquire access to abundant nutrients and become pathogenic, allowing for uncontrolled growth, proliferation and colonization of the lesions. Prior clinical investigations have shown that the pathogens that mostly commonly colonize RDEB skin lesions are *Staphylococcus*, *Pseudomonas*, *Streptococcus*, diphtheroids and *Candida* species.³

Uncontrolled growth of pathogenic microorganisms at a wound site activates the immune system. Innate immunity, particularly neutrophils, plays a leading role in harnessing bacterial infection, however, activation of adaptive T cell-mediated immunity is essential for effective anti-microbial response. Bacterial peptides activate CD4⁺ T helper (Th) cells presented by antigen-presenting cells (APC) in the context of major histocompatibility complex (MHC) class II, enabling effective B cell-mediated immunity and enhancing clearance of the pathogens. Cytotoxic CD8⁺ T lymphocytes (CTL) also help to clear some microbial infection. Unlike Th cells, CTL recognize antigens (Ag) presented in the context of MHC class I (MHC I) molecules. Although CTL are commonly activated after viral infections, several studies showed that bacterial Ag could undergo MHC I restricted CD4⁺ and CD8⁺ T cells priming and activation if bacteria could escape intracellular lysis and survive inside the host.⁴ Yet, only professional antigen presenting cells (APC), such as epidermal Langerhans cells (LC) and dermal dendritic cells (DC), could activate MHC class I-restricted adaptive T cell-mediated immunity.

Little is known about the state of the adaptive immunity in RDEB skin wounds. We recently established an experimental protocol that enabled isolation of wound bed-associated cellular and molecular constituents, and we demonstrated that RDEB wound progression is associated with the accumulation of CD80⁺CD86⁺ mature APC, antigen-experienced CD45RO⁺ peripheral memory T cells and their transition to CD45RA⁺ effector cells.⁵ In this study, we investigated the status of T cell-mediated immunity in RDEB lesions and its contribution to harnessing microbial pathogens.

2 | MATERIALS AND METHODS

More detailed experimental procedures are described in Supporting Information and Methods.

2.1 | Subjects and samples

Regulatory approval for the collection of patient material has been obtained from the local ethics committee and is in accordance with local laws and regulations for the protection of human subjects. All patients received counselling pertaining to the study, and written informed consents were obtained from all patients or their legal guardians. Information on wounds and patients from which dressings were collected is provided in Supporting Information Table S3.

2.2 | Isolation of wound associated cells from wound dressing

RDEB wound-associated cells were isolated from wound-covering bandages as described previously.⁵ CD3⁺ pan T cells were isolated using positive selection following expansion using Immunocult media supplemented with IL-2 and T-cell activator (Stem Cell Technologies, Cambridge, MA).

2.3 | Immuno-phenotyping and fluorescence-activated cell sorting analyses

RDEB wound-derived and control T cells isolated from peripheral blood of healthy donors (about 5×10^4 cells/sample) were incubated with fluorophore-labelled leukocyte marker-specific antibodies (BioLegend, San Diego, CA) for 30min at +4°C. Fluorescence was assessed by fluorescence-activated cell sorting (FACS) on the Guava EasyCyte system and analysed using GuavaSoft 2.7 software (Millipore, Billerica, MA).

2.4 | Preparation of microbial antigens

Samples of the wound-populating microbiota were collected from transport media during isolation of cellular constituents.⁵ All collected media was filtered through 0.22 µm filters, and filters were intensively scraped in PBS. To obtain pooled soluble antigens, the resultant bulk microbiota samples or *Staphylococcus aureus* (Invitrogen, Carlsbad, CA) were heat inactivated at 95°C for 1 h. Concentration of the resultant antigenic mixture was assessed calorimetrically using 660 reagent (Thermo/Fisher, Waltham, MA).

2.5 | Intracellular cytokine staining

Analysis of IL-2 and IFN γ induction in T cells was performed on antigen-exposed and control T cells (1×10^5 cells/reaction) using ICS detection kit with brefeldin A (Golgiplug; BD Bioscience, San Jose, CA) according to the manufacturer protocol. Cytokines, CD4, CD8 and CD107a were detected using protein-specific antibodies (BioLegend). Stained cells were evaluated and analysed on Guava EasyCyte FACS System (Millipore).

2.6 | ELISA-based quantitation of cytokine release

Analysis of cytokine secretion from T cells was done using Quantikine cytokine-specific ELISA (IFN γ , IL-2, IL-17), according to manufacturer protocol (R&D Systems, Minneapolis, MN).

2.7 | T-cell stimulation

RDEB-derived and control T cells were incubated with Ag ($50 \mu\text{g}/\text{ml}$) in Immocult-XL media (Stem Cell Technologies). At variable time points, media and cells were collected for the analyses of cytokine secretion and T-cell activation status by FACS. Micrographs of the proliferating T cells were taken during observational period.

2.8 | T-cell proliferation assay

T-cell proliferation was evaluated by the standard CFSE dilution assay. Cells were labelled with CFSE according to manufacturer protocol (Invitrogen). Labelled T cells were exposed to microbial Ag for various times, and samples were collected to define CFSE dilution (changes in mean fluorescence intensity) using Guava EasyCyte FACS System (Millipore).

2.9 | Analysis of the microbial contaminants

Microbial contaminants were identified by PCR using species-specific primers (Table S1). To evaluate microbial contaminants in exudates and media from cultured wound-derived cells, liquids were filtered through $0.22 \mu\text{m}$ nylon filters that were then crashed and boiled in H_2O for 15 min to recover DNA. To define intracellular bacteria, wound-derived cells were cultured for 48 hr in HighBind 48-well plates. Then, cells were washed twice in acid buffer (pH 3.0) to remove unbound bacteria (*S. aureus*) and twice in PBS. Cell pellets were resuspended in $150 \mu\text{l}$ H_2O and boiled for 15 min to recover DNA. Recovered total DNA was used for PCR (100 ng per reaction).

2.10 | Indirect immunofluorescence and confocal microscopy

Indirect immunofluorescence (IFC) was done using standard protocol. A list of antibodies, dilutions, source and catalogue number are provided in Table S2. Images were acquired on an inverted fluorescent microscope and analysed using NIS elements software (Nikon TS100; Melville, NY). To evaluate bacterial infectivity and intracellular *S. aureus* routing, cells were incubated in serum-free EpiLife media without calcium and magnesium (Thermo/Fisher) for 2 h. Then, inactivated, fluorescently-labelled *S. aureus* (Invitrogen) was added to cultures (1×10^6 particles/ml) for 4 h or overnight. After extensive washes, cells were fixed in 4% PFA and subjected for IFC detection of the intracellular structures using protein-specific antibodies. Slides were imaged on confocal Zeiss LSM780 NLO confocal microscope and analysed using Zeiss LSM imaging software (White Plains, NY).

2.11 | *S. aureus* uptake by keratinocytes

Control and RDEB-derived keratinocytes (Supporting Information Table S4) at 90% confluence were infected with AlexaFluor⁵⁹⁴-labelled inactivated *S. aureus* (Wood strain; Invitrogen/Molecular Probes; 6×10^6 bacterial particles per well). Cells were exposed to bacteria for designated periods. After infection, cells were extensively rinsed with citric acid buffer (pH 4.4) and PBS. Wells were covered with FluorSafe reagent (Calbiochem/Millipore).

2.12 | Multiplex cytokine and chemokine analysis

Secretion of pro-inflammatory chemokines (CCL2, CCL3, CCL4, CCL5, CCL11, CCL17, CCL20, CXCL1, CXCL5, CXCL9, CXCL10, CXCL11) and cytokines (TNF- α , MCP-1, IL-6, IL-8, IL-10, IL-12, IL-17, IL-18, IL-23, IL-33) in culture media from antigen-exposed and control T cells was done using LegendPlex MultiPlex ELISA (Biolegend). Control and RDEB-derived T cells were cultured in the presence or absence of soluble *S. aureus* antigens for 72 and 120h. Then, culture media was clarified by subsequent centrifugation at 300 and 10 000g to remove cells and debris, respectively. Twenty-five microlitres of clarified media were used for MultiPlex ELISA according to manufacturer protocols.

2.13 | Statistical analysis

Comparison of the data was performed using Student 2-tailed t-test; $p < 0.05$ was considered statistically significant.

3 | RESULTS

3.1 | Wound-associated *S. aureus* could serve as a common target for T cell-mediated immunity in RDEB skin

To define microbial species whose antigens could be recognized by the adaptive T cell-mediated immunity, we evaluated extracellular and intracellular microbial contaminants in cellular fraction and exudates obtained from RDED wounds with no documented active infection, as described previously.⁵ The samples were subjected to PCR-based analysis of the most common microbial contaminants identified in RDEB wounds⁶ with species-specific primers (Table S1). This evaluation showed that *S. aureus* is detected in more than 50% of the exudates ($n = 57$) with high, medium and low levels of contamination as defined by semi-quantitative PCR, whereas *Staphylococcus epidermidis* and *Pseudomonas aeruginosa* were detected in a substantially lower percent of samples with mostly high and medium levels of infection (Figure 1A,B). Other examined bacterial and fungal contaminants (Table S1) were not detected. When bandage-derived cells were placed in culture conditions, one-third of samples showed the presence of *S. aureus* either in conditioned media or intracellularly (Figure 1C,D). These findings demonstrated that *S. aureus* can infect and survive in keratinocytes at RDEB wounds.

Unlike viruses which most often utilize cell surface receptors to infect the host, bacteria are engulfed by the host cells. Macrophages and neutrophils are well-equipped for bacterial phagocytosis. However, studies have shown that other cell types, particularly keratinocytes, could engulf the bacteria.^{7,8} Using AlexaFluor⁵⁹⁴-labelled *S. aureus*, we evaluated its ability to infect control and RDEB-derived keratinocytes. Our assessment showed that overnight exposure of the cells to bacteria leads to a more robust infection of RDEB- (6-times) and RDEB-associated squamous cell carcinoma (RDEB SCC)-derived (10-times) keratinocytes with *S. aureus* when compared with keratinocytes from healthy donors (Figure 1D). Using confocal microscopy to scan infected cells at 5 μm Z-position, we observed an overwhelming intracellular presence of bacterial particles in the RDEB cells. In control keratinocytes, bacterial particles were mostly detected on cell surface (Figure 2A). *S. aureus* co-localization with Rab7⁺ endosomes was very prominent in RDEB SCC (Figure 2B). Further analysis of the intracellular bacterial trafficking showed that *S. aureus* could be detected in association with LC3⁺ autophagosomes (Figure 2C) and routed toward LAMP2⁺ phagolysosomes (Figure 2D).

3.2 | Microbial antigen-specific CD4⁺ and CD8⁺ T cells are present in RDEB skin wounds

To evaluate whether microbial antigen-specific CD4⁺ and CD8⁺ T cells are present in RDEB skin wounds, we isolated a pool of CD3⁺ T cells by positive selection from bandage-derived leukocytes and propagated them in vitro. FACS-based immuno-phenotyping showed

that CD4⁺ and CD8⁺ T cells are present in the CD3⁺ population at an average ratio of 6 to 1 (Figure 3A). Exposure of RDEB-derived T cells to wound-associated pooled microbial Ag led to clonal expansion that was most prominent after 48h of exposure (Figure 3B). CFSE dilution assay confirmed these observations by showing that 2-day exposure to microbial Ag induced vigorous proliferation in about 30% of RDEB wound-derived T cells and did not substantially affect proliferation of control T cells in which anti-CD3/CD28 stimulation triggered robust proliferation (Figure 3C). Intracellular staining for IFN γ combined with detection of CD107a degranulation marker confirmed microbial Ag-specific T-cell activation in RDEB T cells ($n = 5$). Two days of exposure induced IFN γ expression in about 50% of RDEB T cells, whereas induction of IL-2 was detected in only 10% of cells (Figure 3D,F). Quantitative ELISA showed a significant increase in IFN γ secretion from RDEB T cells detected at 100pg/ml after 1 day of exposure and 275pg/ml after 7 days of exposure (Figure 3E). However, analysis of IL-2 and IL-17 in culture media did not display any appreciable secretion of these cytokines. Population profiles showed the presence of a small CD107a^{high}IFN γ ^{high} population of T cells that was identified as CD8⁺ T cells (Figure 3E). Collectively, these data demonstrated that RDEB wounds contain a pool of primed T cells that react to microbial antigens by proliferation, degranulation and secretion of IFN γ .

3.3 | Wound-derived T cells can recognize *S. aureus* antigens and target infected keratinocytes in HLA-dependent manner

Considering our findings that *S. aureus* infects RDEB cells and that the presence of *S. aureus* super antigens could activate adaptive immunity,^{9,10} we tested the capacity of RDEB T cells to recognize and target *S. aureus*-infected keratinocytes. To set-up an IFN γ ELISpot assay, we screened five primary RDEB-derived keratinocyte cell lines and patient-derived T cells ($n = 5$) for HLA-A02.1 and HLA-A03.1 expression for HLA matching (data not shown). *S. aureus*-infected and uninfected keratinocytes were used as targets and control and RDEB T cells were used as effectors. Exposure of control or patient-derived T cells to soluble *S. aureus* Ag slightly increased a number IFN γ spot-forming cells (SFC) (Figure 4A). Minor activation of control and RDEB T cells in response to uninfected keratinocytes was attributed to allogeneic response. Yet, a significantly greater number of SFC were detected when RDEB T cells were exposed to *S. aureus*-infected RDEB keratinocytes as compared with control (Figure 4A). T cells isolated from established RDEB lesions contained significantly greater number of IFN- γ -producing T cells than T cells from early and chronic lesions. IL-2 and IFN- γ intracellular staining combined with detection of the CD107a degranulation marker confirmed that a significantly higher percentage of cytokine-expressing RDEB T cells responded to *S. aureus* (Figure 4B). CTL capable of targeting and killing infected keratinocytes were also identified among RDEB T cells (Figure 4C). Moreover, CTL response to infected cells appeared to be HLA-restricted. Four independent patient-derived

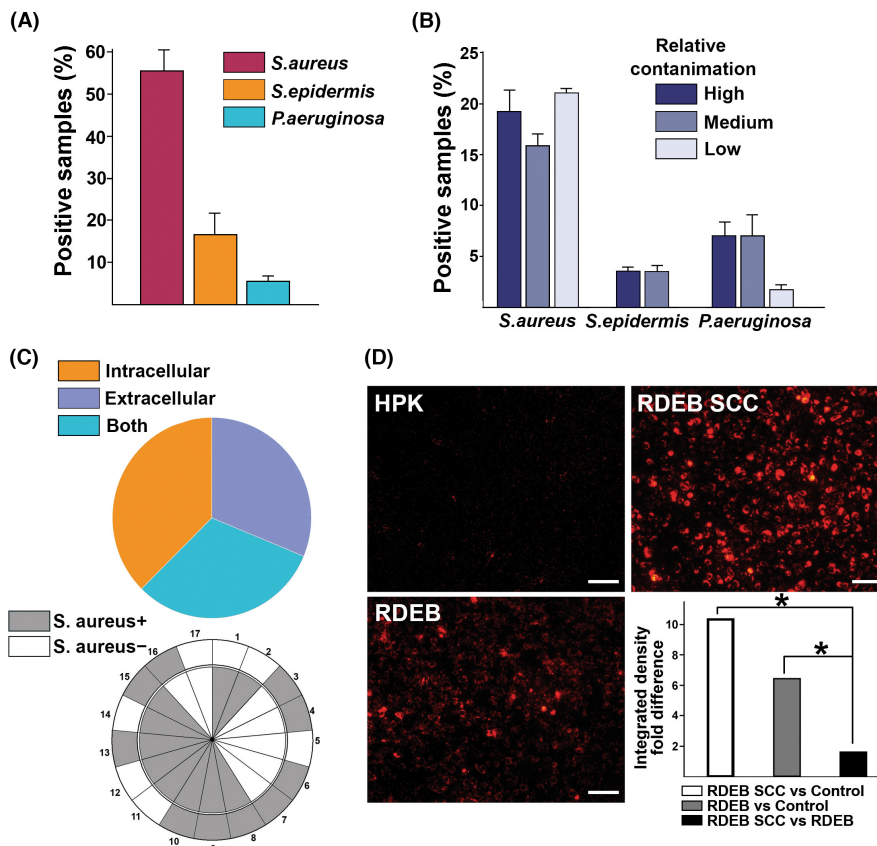


FIGURE 1 Analysis of bacterial infection in RDEB wounds and keratinocytes. (A) Analysis of most common bacterial contaminants and (B) relative percentage of contamination of RDEB wound exudates ($n = 57$) detected by bacteria-specific PCR. Data are presented as percent of bacteria-positive samples assessed in triplicate independent measurements \pm SD. (C) Pie charts illustrating ratio of intracellular and extracellular *S. aureus* in analysed samples ($n = 37$; top chart) and in a group of samples ($n = 17$) of bandage-recovered cells in tissue culture conditions. In the bottom chart, outer circle—extracellular fraction (culture media); inner circle—cellular fraction. Positive and negative samples are shown in the key to the chart. (D) Representative micrographs depicting infectivity of a monolayer culture (90% confluence) of human primary keratinocytes (HPK), primary RDEB keratinocytes and primary keratinocytes from RDEB squamous cell carcinoma (RDEB SCC) with fluorescently-labelled *S. aureus* (red). Quantitation of fluorescent signals (mean fluorescence intensity [MFI]) was done on 5 independent microscopic fields and presented on a column chart as fold difference between MFI average in control and RDEB cells, as indicated. Fluorescence intensity was normalized by the level of background fluorescence. Scale bar-100 μ m. Single channel images are presented in Figure S1

HLA-A02⁺ T cells showed higher CTL activity towards HLA-A02⁺ *S. aureus* infected targets. One of these T-cell pools, while having specific CTL activity against HLA-A02⁺ targets, showed unspecific allogeneic response towards HLA-A3⁺ targets. Conversely, HLA-A03⁺ patient-derived T cells were more specific against HLA-A03⁺ than towards HLA-A2⁺ infected targets (Figure 4C). Evaluation of pro-inflammatory chemokines and cytokines showed that 72h exposure of RDEB-derived T cells to *S. aureus* antigens induces secretion of CCL5, CCL3 and CCL11, which coincided with down-regulation of IL-12 and IL-10. Additional 48h of exposure did not significantly alter secretion of the chemokines, yet, a significantly higher levels of IL-10 were detected (Figure 4D). Comparison between T cell isolated from early, established and chronic wounds did not reveal substantial differences in secretion of cytokines or chemokines, although somewhat higher IL-10 levels were produced by T cells isolated from chronic wounds. Conversely, lower secretion of CCL5 and CCL3 and higher secretion of CCL4 and IL-12 were detected in

antigen-exposed control T cells (Figure 4D). No changes in other examined chemokines and cytokines were detected. Collectively, these data demonstrated that *S. aureus*-specific memory/effector T cells capable of producing IL-2 and IFN- γ and killing infected keratinocytes are present in RDEB wounds. These data also point out that exposure of RDEB wound-derived T cells leads to the secretion of chemokines and cytokines that influence on T-cell responses.

3.4 | PD-1 and Treg-dependent mechanisms may contribute to inhibition of bacterial antigen-specific T cells in chronic RDEB wounds

In chronic infections, T cells exposure to persistent antigenic load could result in down-modulation of robust T cell effector function via activation of programmed cell death protein 1 (PD-1) and T cell exhaustion or through induction of regulatory T cells (Treg).¹¹⁻¹³

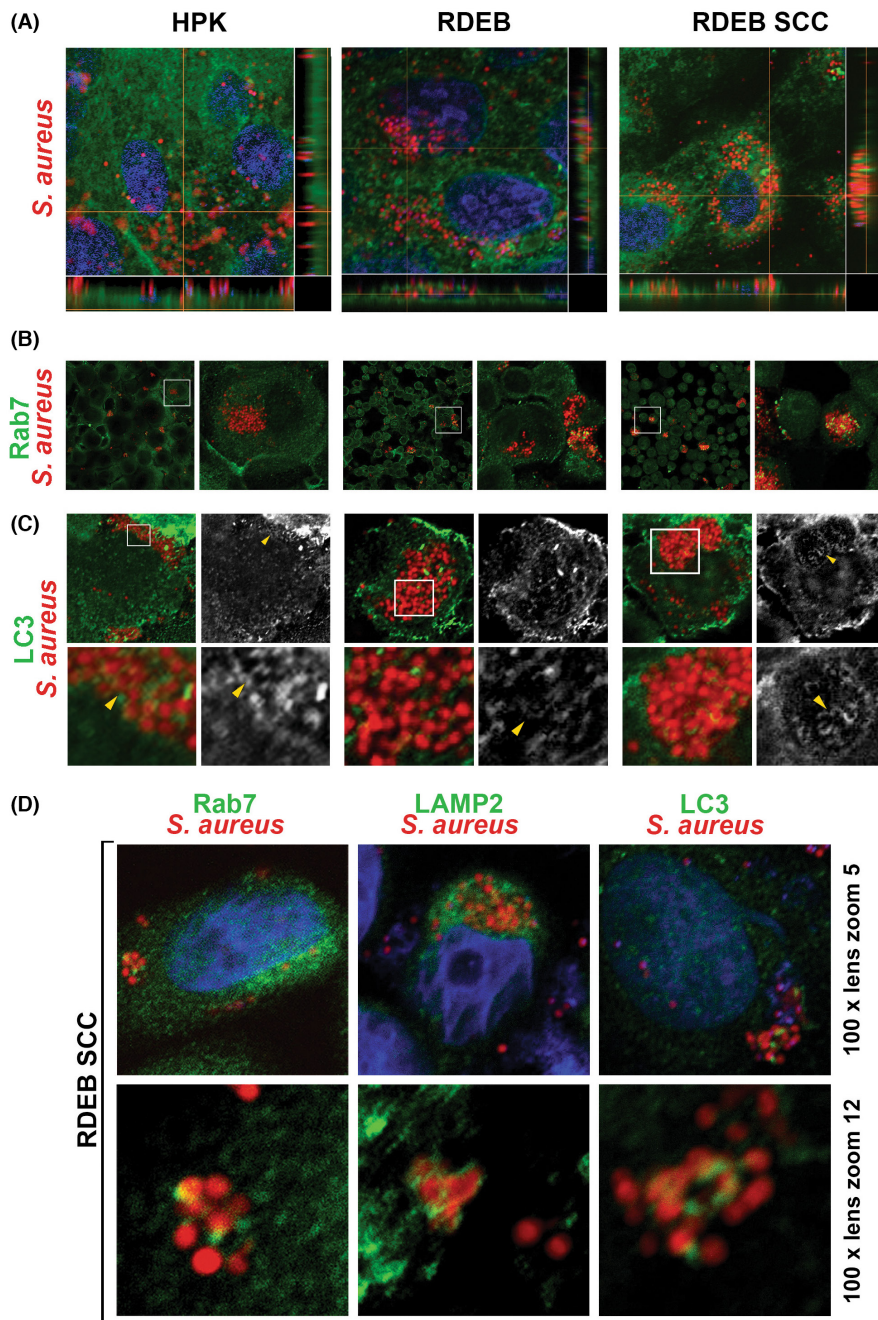


FIGURE 2 Analyses of the infectivity and the intracellular trafficking of the *S. aureus* in control and RDEB keratinocytes. (A) Images of confocal scanning microscopy of Vibrant DiO-labelled (green) human primary keratinocytes (HPK; control), RDEB keratinocytes and RDEB SCC keratinocytes infected with *S. aureus* (red) at 5 μm Z-position illustrating intracellular location of *S. aureus* in cells after overnight infection. (B, C) Micrographs illustrating co-localization of the intracellular *S. aureus* (red) with Rab7⁺ (B) and LC3⁺ (C) endosomes (green) in control and RDEB keratinocytes (indicated above the micrographs) after overnight infection. Detected antigens are colour-coded and shown to the left of the panels. Areas with typical co-localization are shown on magnified fields. Yellow arrowheads point to representative *S. aureus*⁺ endosomes (B&W images, green channel). (D) Representative magnified confocal images (5 μm Z-position) of *S. aureus* (red) routed from Rab7⁺ endosomes to LAMP2⁺ phagolysosomes and LC3⁺ autophagosomes (green) in RDEB-SCC keratinocytes. Magnification is shown to the right of the micrographs. Detected antigens are colour-coded and shown above the micrographs. Blue-DAPI nuclear staining. In all images, co-localization is detected as overlapping red/green signals (yellow). All images are representative. Single channel images are presented in Figure S2

One-day exposure of RDEB T cells to the pooled microbial Ag led to induction of PD-1 expression on about 20% of the cells with no substantial differences in the CD8⁺ T-cell population (Figure 5A). By day 2, the CD69 T-cell activation marker was induced along with PD-1 on about 30% of CD4⁺ T cells. By day 3, about 60% of CD4⁺ T cells were identified as CD69⁺PD-1⁺ cells. However by day 6, CD69 expression was diminished, yet, about 60% of CD4⁺ T cells continue to express PD-1. During the observed period, no induction of CD57, a marker of PD-1-mediated T-cell exhaustion, was detected in control (not shown) and RDEB T cells (Figure 5B). Exposure to pooled *S. aureus*-derived Ag for 2 days also triggered prominent PD-1 expression in about 40% of RDEB T cells, a level of expression that was significantly higher than in control T cells (Figure 5C). However, 6 days

of exposure of both T cell types led to PD-1 expression in more than 60% of T cells. Unlike exposure to pooled microbial Ag, exposure to *S. aureus* Ag led to a separation resulting in two distinct populations with lower and higher levels of CD4. The entire CD4^{high} population was PD-1 positive (Figure 5C). CD57 was expressed on only 2% of RDEB T cells.

To test whether the interaction of T cells with MHC-presented Ag triggers a similar response, we infected RDEB SCC keratinocytes with inactivated *S. aureus* and exposed them to T cells. After 6 days of exposure, PD-1 expression was induced in control and RDEB-derived T cells up to 50% and 80%, respectively. CD57 expression was detected in about 2% of PD-1⁺ T cells (Figure 5D). No separation of CD4⁺ T cells into 2 distinct populations was detected. Suggesting

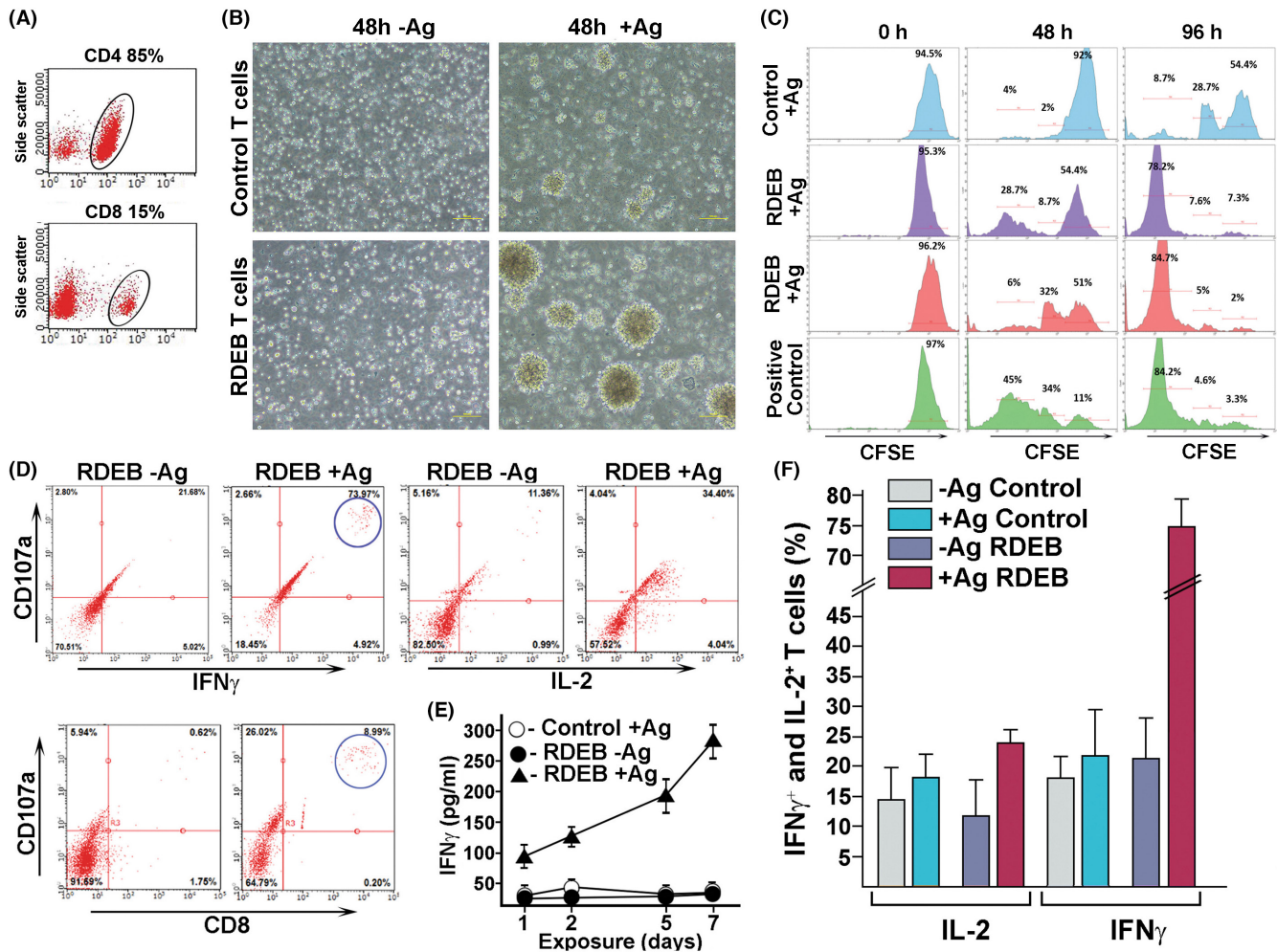


FIGURE 3 Analysis of T-cell responses to pooled RDEB wound-derived microbial antigens. (A) Density plots illustrating FACS-based evaluation of CD4⁺ and CD8⁺ T cells (outlined populations) recovered from RDEB wounds. Percentages are shown above the plots. (B) Micrographs of control and RDEB wound-derived T cells illustrating clonogenic proliferation of RDEB cells after 48h of exposure to pooled microbial antigens. (C) Representative FACS profiles depicting T-cell proliferation defined by CFSE dilution assay. Time of exposure to microbial antigens is shown above the profiles. Percentages of proliferating and non-proliferating cells are indicated on plots. Experimental conditions are shown to the left of the plots. Positive control—T cells activated with anti-CD3/CD28 in the presence of IL-2. (D) Density plots showing induction of the IL-2 and IFN γ in RDEB-derived T cells after 5 h of exposure to microbial antigens. Conditions are shown above the plots. Detected antigens are shown on x- and y-axes. Population of CD8⁺ IFN γ ⁺ CD107a⁺ T cells is outlined. (E) Graph showing ELISA-based quantitation of IFN γ secretion from T cells exposed to microbial antigens, as indicated in the key. (F) Quantitation of IL-2 and IFN γ induction in T cells exposed to microbial antigens, as indicated in the key. Data are presented as an average of percentages of cytokine-positive cells from 3 independent measurements \pm SD. Detected cytokines are shown below the columns

that PD-1 could be activated by PD-1 ligand (PD-L1) expressed by infected keratinocytes, we evaluated its expression in infected and non-infected RDEB SCC. Indirect immuno-fluorescence and Western blot analyses showed no significant induction of PD-L1 in the cells after infection. However, in uninfected RDEB cells, PD-L1 was detected mostly intracellularly, whereas in infected cells, it was localized to the membrane as defined by light and confocal microscopy (Figure 5E).

Since immune-inhibitory activity of regulatory T cells (Treg) may also play a role in diminishing T cell-mediated response,¹¹ we evaluated the presence of Treg in control and RDEB T cells in similar settings. FACS-based analysis showed that both control

(not shown) and RDEB T cells contain a small (~2%) population of CD4⁺CD25⁺FOXP3⁺ Treg among CD4-gated T cells and that this percentage was increased after 6 days of exposure to microbial and *S. aureus* Ag up to 10% in the control and 20% in the RDEB T cells (Figure 5F). The majority of CD25⁺FoxP3⁺ Treg were identified in the CD4^{high} population (Figure 5F). When T cells were exposed to *S. aureus*-infected keratinocytes for 6 days, much lower (i.e., up to 7%) induction of Treg was detected in the RDEB T cells (Figure 5F). No substantial Treg induction was detected in control T cells (not shown). All detected differences between control and RDEB T cells to microbial, *S. aureus* and *S. aureus*-infected keratinocytes were significant (Figure 5G).

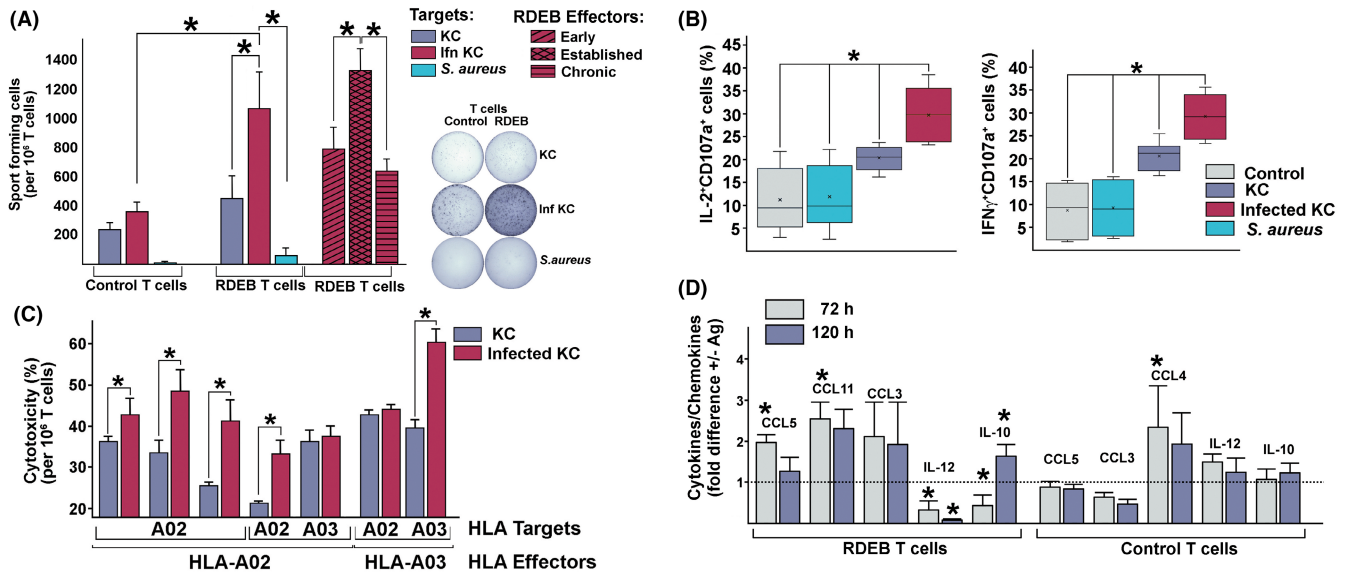


FIGURE 4 Analysis of T-cell activity against *S. aureus*-infected keratinocytes. (A) Quantitation and representative images of IFN γ spot forming cells exposed to *S. aureus*-infected keratinocytes (KC) and *S. aureus* pooled antigens, as indicated in the key. T cells used for analysis are shown below the columns. Activation of T cells (IFN γ SFC) from early, established and chronic RDEB wounds (Effectors; indicated in the key) exposed to infected keratinocytes were evaluated separately. Data are presented as mean \pm SD. (B) Box and whiskers plots showing induction of IL-2 and IFN γ expression along with degranulation (CD107a⁺) in RDEB T cells incubated with RDEB keratinocytes (KC), infected RDEB KC and *S. aureus*, as shown in the key. Mean values and SD are shown on plots. (C) Column chart illustrating cytotoxic activity of RDEB wound-derived T cells exposed to uninfected and *S. aureus*-infected KC, as indicated in the key. Data is presented as an average cytotoxicity (%) at fixed effector: target (E:T) ratio 50:1 \pm SD. Data was acquired in 5 independent experiments using HLA-A02⁺ and HLA-A03⁺ (as indicated) RDEB KC ($n = 3$) as targets and RDEB T cells ($n = 5$) as effectors. (D) Column chart illustrating changes in cytokines and chemokines (shown above the columns) secreted by RDEB and control T cells (indicated below the charts) 72 and 120h of exposure to *S. aureus* pooled antigens (indicated in the key). Data are presented as an average fold-difference to levels in control media (collected from control cells, indicated by dotted line) \pm SD. Significance is indicated by asterisk

4 | DISCUSSION

It is well known that skin wounds of RDEB patients are frequently colonized by bacteria and fungi that impare wound healing. Critical colonization leads to increased wound size, pain, erythema and development of chronic wounds.^{3,6} Yet, the role of innate and adaptive immunity in controlling microbiota in RDEB-associated wounds remains incompletely understood. Recently, animal studies demonstrated that poor control of infection in RDEB wounds could be associated with altered macrophage activity due to lower levels of cochlin in the circulation.¹⁴ However, it is plausible that inaptitude of the immune system to control wound infection could be caused by other post-infectious immunopathology in RDEB skin.

In support of this notion, we previously demonstrated that blister formation coincides with increased levels of CXCL2, CCL2, CCL4 and CCL5 and with elevated recruitment of granulocytes and T cells.¹⁵ Furthermore, we showed that progression of RDEB wounds to an established and chronic state is accompanied by reduction of macrophages, continuous recruitment of mature neutrophils, accumulation of antigen-experience APC and differentiation of peripheral memory T cells into effector T cells.⁵ Thus far, functional activity of adaptive T cell-mediated immunity remains uncharacterized in RDEB skin lesions. Based on our current knowledge, we proposed that RDEB wound-associated APC play a role in the

acquisition of microbial antigens, T-cell priming and activation as it was shown for naïve T cells that differentiate into effector and memory T-cell pools¹⁶ and support B cell-mediated antibody response and innate immunity to clear bacterial contamination.¹⁷ Consistent with this notion, data presented here showed that RDEB wounds contain antigen-experienced CD4⁺ T cells that proliferate and secrete IFN γ , a potent activator of polymorphonuclear neutrophils (PMN)¹⁸ in response to microbial antigens. Higher number of IFN γ -producing T cells in established RDEB wounds (Figure 4A) correlates extremely well with our prior data demonstrating accumulation of differentiated PMN to these advanced RDEB lesions.⁵ T cell-derived IFN γ is also heightens macrophage response to microbial products and is a potent inducer of macrophage M1 polarization.¹⁹ However, paucity of the macrophages in RDEB advanced skin lesions detected in our prior studies⁵ and impaired macrophage response in infected RDEB wounds¹⁴ suggest that T cell-derived IFN γ primarily activates PMN in RDEB lesions. Reduction of IFN γ -producing T cells in chronic RDEB wounds (Figure 4A) suggests inadequate IFN γ -mediated PMN stimulation and their functional impairment in chronic lesions.

Besides detecting CD4⁺ Th cells, we have identified a small population of CD8⁺ CTL among RDEB wound-associated T cells. Although the role of CTL in harnessing bacterial infection in the skin, and particularly in RDEB wounds, remains poorly defined, we suggest that bacterial Ag-specific CTL could target host cells

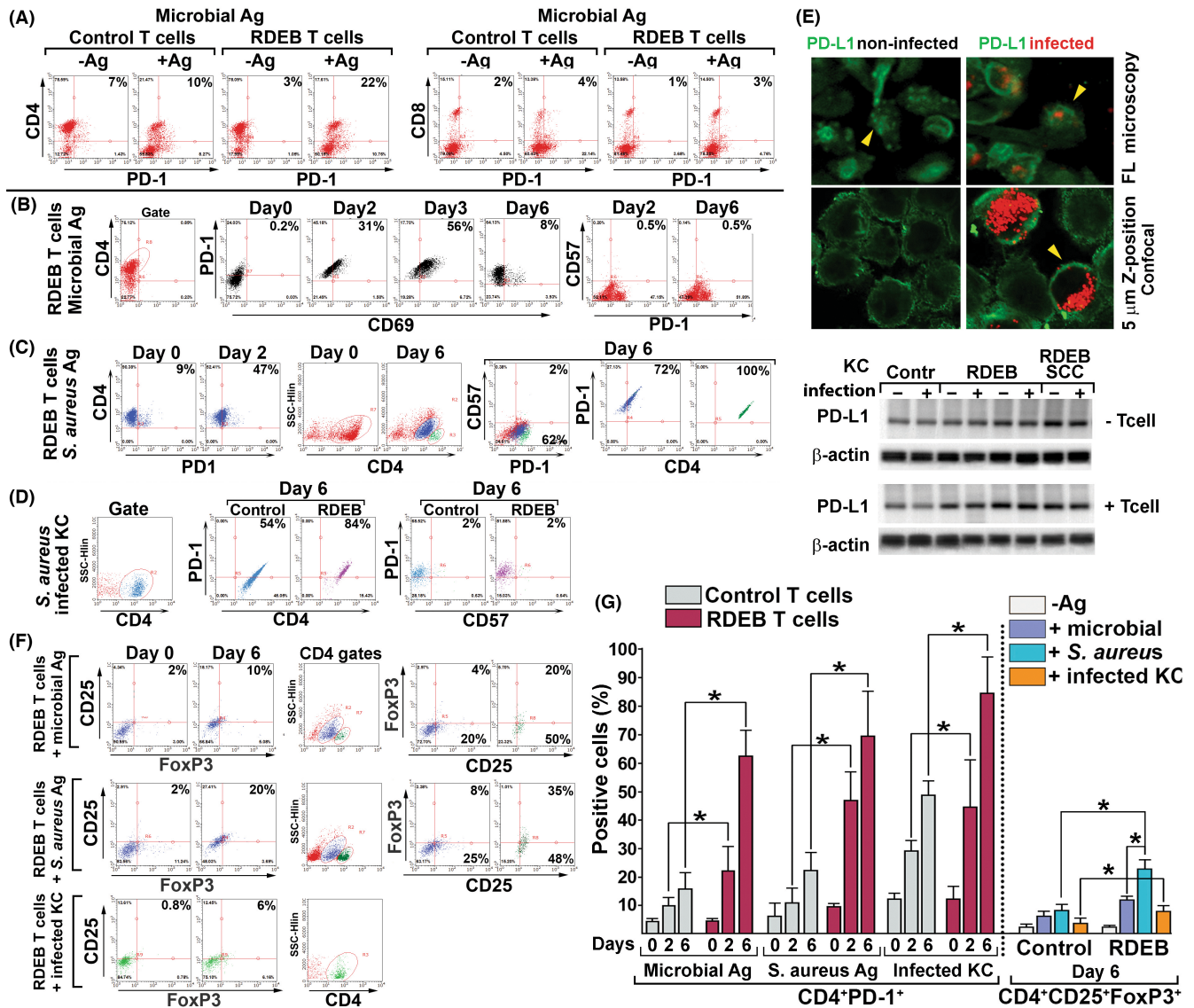


FIGURE 5 Analysis of RDEB-associated putative microbial infection-induced T-cell impairment mechanisms. (A–D) Representative dot plot flow cytometry analysis of PD-1, CD57 and CD69 expression (as indicated) in control and RDEB-derived CD4 and CD8 T cells illustrating T-cell responses to RDEB wound-derived pooled microbial antigens (A, B), pooled *S. aureus* antigen (C) and *S. aureus*-infected RDEB keratinocytes (D). In all plots, detected T-cell markers are shown along y- and x-axes, percentages of double-positive T cells are shown in a top right quadrant. Days of sample collection after exposure to the indicated microbial antigens (Ag) are shown above the plots. In (C), middle plots illustrate differentiation of CD4⁺ population into 2 distinct CD4⁺ (blue) and CD4^{high} (green) populations. Far right plots show expression of PD-1 in CD4⁺ and CD4^{high} T-cell populations. (E) Indirect immunofluorescence and Western blot (WB) analyses of PD-L1 (green) expression in *S. aureus* (red)-infected and non-infected RDEB keratinocytes (KC; as indicated). Representative micrographs and WB illustrate no PD-L1 induction in infected control, RDEB and RDEB SCC KC. WB shows that PD-L1 expression did not depend on either infection or T cells presence. Accumulation of PD-L1 on the membrane was observed after infection. Yellow arrowheads on micrographs point to the cells exemplifying this effect. (F) Representative flow cytometry plots illustrating differentiation of CD4⁺CD25⁺FoxP3⁺ Treg cells 6 days after exposure to pooled microbial Ag, *S. aureus* Ag, and *S. aureus*-infected RDEB KC (as indicated to the right of the plots). Plots in the middle depict typical differentiating of the T cells into CD4⁺ and CD4^{high} populations 6 days after exposure to microbial and *S. aureus* Ag, and a lack of such differentiation after exposure of T cells to infected KC. Plots to the right illustrate that the majority of Treg cells are present in the CD4^{high} population. In all plots, percentages of specific populations are shown in quadrants, and detected T-cell markers are indicated on x- and y-axes. (G) Column chart summarizing all analyses and showing statistically significant differences ($p < 0.05$, indicated by asterisk) between different T-cell populations (as indicated). Days of exposure and antigens are shown below the columns. Types of T cells and antigens are colour-coded as shown in the key. Single channel images are presented in Figure S3

in which bacteria evade intracellular destruction. Such a situation has most frequently been described for professional phagocytes, such as macrophages.^{20,21} Bacteria have diverse mechanisms for

avoiding autophagy,²² including escaping to cytoplasm where they can survive and replicate. Such escape leads to the introduction of bacterial antigens into the cytoplasmic compartment and MHC class

I-mediated presentation, making bacterial Ag "visible" to the CTL. Although this mechanism was described for some bacterial and protozoan infections more than 30 years ago,²³ only recently have we started to learn about the intracellular behaviour of the majority of bacterial species in vivo. Thus, several studies have shown that keratinocytes could engulf bacterial particles and that bacteria (e.g., *S. aureus*) could escape into the cytoplasm by inhibiting autophagosome maturation.⁸

Among others, *S. aureus*, as one of the most frequent skin colonizers, was associated with progression of keratinocyte skin tumours. Clinical studies have shown that this bacteria frequently infects pre-malignant actinic keratosis and cutaneous SCC.²⁴⁻²⁶ Our data corroborate these findings in showing significantly higher susceptibility of the RDEB SCC to *S. aureus* infection and suggesting that malignant transformation of the cells could modulate bacterial engulfment. Although the exact mechanism of *S. aureus* engulfment by SCC remains to be further elucidated, it is plausible that some sphingolipids that are associated with advanced stage of SCC²⁷ play an important role in bacterial engulfment via "lipid zippering," a mechanism described for *P. aeruginosa* infection.²⁸ Moreover, identified association of the *S. aureus* particles with both LAMP2⁺ phagolysosomes and LC3⁺ autophagosomes suggests that, in RDEB keratinocytes, bacteria could be routed to degradation or escape to the cytoplasm.⁴ In the latter scenario, adaptive immunity could recognize bacterial antigens presented in the context of MHC I by specific T-cell receptors developed against MHC-antigenic peptide complex. This concept is directly supported by our data showing typical T-cell responses towards *S. aureus*-infected keratinocytes (Figure 4). Of particular note are elevated CTL activity towards infected cells and significant induction of both IFN γ and IL-2 after exposure of T cells to infected keratinocytes. This is contrary to the lack of IL-2 response to soluble microbial antigens, where only IFN γ induction and secretion were significant (Figure 3). Considering that *S. aureus*-derived super-antigens could activate T cells in orders of magnitude above conventional process,²⁹ it is plausible that a full array of T-cell activities could be engaged only against MHC I-mediated presentation of bacterial Ag and that exposure of peripheral memory T cells to soluble microbial Ag is limited to IFN γ production to support PMN activity.

In chronically infected wounds, T cells are often exposed to persistent antigenic load and inflammatory signals, resulting in over-stimulation and T cell exhaust and/or Treg-mediated immunosuppression.¹² Our experiments showing transient induction of CD69, persistent expression of PD-1 in T cells exposed to microbial Ag and infected keratinocytes and a lack of CD57 induction within 6 days of exposure suggest that PD-1-mediated exhaustion may not be the primary mechanism of the T-cell inhibition. Nevertheless, presented data showing that the CD4^{high} T cells differentiate into CD25⁺FoxP3⁺ Treg cells upon exposure to pooled microbial and *S. aureus* Ag but do not differentiate in experiments involving infected keratinocytes (Figure 5F) suggest that soluble microbial Ag at wounded sites could induce Treg and provide a primary immunosuppressive effect. Because the CD4^{high} population almost uniformly

expresses PD-1 (Figure 5C), it is plausible that PD-1 expression synergizes with Treg-mediated inhibition³⁰ and enhances suppression of the CD8⁺ T-cell responses, as it was shown in chronic viral infection and neoplasms.³¹ Our findings showing that RDEB wound-derived T cells could present their anti-microbial activity ex vivo within 7 days of exposure and that PD-1⁺ Treg cell differentiation during the same period suggest that synergistic Treg-PD-1-mediated inhibition of T-cell immunity could be a conservative mechanism that extends to cutaneous bacterial infection. These findings also indicate that revitalization of exhausted T cells or inhibition of Treg differentiation could re-invigorate anti-bacterial T cell-mediated immunity in RDEB wounds and, potentially, prevent bacterial survival in the host and RDEB-associated SCC progression via immune-mediated elimination of infected malignant cells. Activation of T cells by microbial antigens and inhibition of this response after prolonged exposure is also supported by secretion of pro-inflammatory chemokines and cytokines by *S. aureus* antigen-exposed RDEB T cells. This is illustrated by reduced secretion of the immune-inhibitory cytokine IL-10 during first 2.5 days of antigen exposure and induction of this cytokine during consecutive 2 days. This process coincides with secretion of T cell-derived CCL11. It is known that CCL11 is expressed by skin-residing T cells and that it is chemotactic to eosinophils that participate in tissue repair and remodelling.³² Very recent studies have shown that CCL11 increases the proportion of CD4⁺CD25⁺FoxP3⁺ Treg cells.³³ This data are in agreement with our findings showing differentiation of RDEB-derived T cells towards FoxP3⁺ Treg upon prolonged exposure to microbial /*S. aureus* antigens (Figure 5).

Although acknowledging that ex vivo and in vitro experimental settings do not recapitulate the complexity of molecular and cellular interactions at wound sites, these studies demonstrated that microbial/*S. aureus*-specific T helper and cytotoxic T cells are present in RDEB skin wounds and that CTL could target infected keratinocytes. Our data indicate that prolonged exposure of wound-associated T cells to soluble microbial antigens and other molecules (e.g., CCL11) could trigger differentiation of Treg cells that could inhibit T cell-mediated immunity at RDEB wound sites.

AUTHOR CONTRIBUTIONS

Taylor Phillips, Leonie Huitema, Julio Cesar Salas-Alanis, Jouni Uitto, Vitali Alexeev, and OI involved in conceptualization. Taylor Phillips, Leonie Huitema, Julio Cesar Salas-Alanis, Vitali Alexeev, and Olga Igoucheva involved in data curation. Taylor Phillips, Leonie Huitema, Vitali Alexeev, and Olga Igoucheva involved in formal analysis. Vitali Alexeev and Olga Igoucheva involved in funding acquisition and project administration. TP, Leonie Huitema, RC, Diego de los Cobos, Regina Isabella Matus Perez, Mauricio Salas-Garza, Oscar R. Fajardo-Ramirez, Franziska Ringpfeil, Julio Cesar Salas-Alanis, Vitali Alexeev, and Olga Igoucheva involved in investigation and resources. Taylor Phillips, Leonie Huitema, Julio Cesar Salas-Alanis, Vitali Alexeev, and Olga Igoucheva involved in methodology. Taylor Phillips, Leonie Huitema, Vitali Alexeev, and Olga Igoucheva involved in software. Taylor Phillips, Leonie Huitema, Vitali Alexeev, and Olga Igoucheva involved in supervision, visualization, validation

and writing—review and editing. Leonie Huitema, Taylor Phillips, Jouni Uitto, Vitali Alexeev, and Olga Igoucheva involved in writing—original draft preparation.

ACKNOWLEDGEMENTS

We would like to thank the Dystrophic Epidermolysis Bullosa Research Association (DEBRA) of Mexico for its efforts to collect patients' samples. Research reported in this publication was supported by the grant from Department of Defence under Award Number W81XWH1810628 to OI.

CONFLICT OF INTEREST

The authors declare no conflict of interest.

DATA AVAILABILITY STATEMENT

The data that support the findings of this study are available from the corresponding author upon reasonable request.

ORCID


Vitali Alexeev  <https://orcid.org/0000-0002-0762-1833>

Leonie Huitema  <https://orcid.org/0000-0003-2947-021X>

Taylor Phillips  <https://orcid.org/0000-0001-9843-4736>

Rodrigo Cepeda  <https://orcid.org/0000-0002-1106-8989>

Diego de los Cobos  <https://orcid.org/0000-0001-6576-6195>

Regina Isabella Matus Perez  <https://orcid.org/0000-0001-9626-8682>

[org/0000-0001-9626-8682](https://orcid.org/0000-0001-9626-8682)

Mauricio Salas-Garza  <https://orcid.org/0000-0003-2076-2312>

Oscar R. Fajardo-Ramirez  <https://orcid.org/0000-0002-7893-8379>

[org/0000-0002-7893-8379](https://orcid.org/0000-0002-7893-8379)

Franziska Ringpfeil  <https://orcid.org/0000-0003-4812-4734>

Jouni Uitto  <https://orcid.org/0000-0003-4639-807X>

Julio Cesar Salas-Alanis  <https://orcid.org/0000-0002-7307-3898>

Olga Igoucheva  <https://orcid.org/0000-0001-9813-7184>

REFERENCES

- Has C, Nystrom A, Saeidian AH, Bruckner-Tuderman L, Uitto J. Epidermolysis bullosa: molecular pathology of connective tissue components in the cutaneous basement membrane zone. *Matrix Biol.* 2018;71-72:313-329.
- Grice EA. The skin microbiome: potential for novel diagnostic and therapeutic approaches to cutaneous disease. *Semin Cutan Med Surg.* 2014;33(2):98-103.
- J.E. Mellerio, Infection and colonization in epidermolysis bullosa, *Dermatol Clin.* 28(2) (2010) 267-9, ix.
- Huitema L, Phillips T, Alexeev V, Tomic-Canic M, Pastar I, Igoucheva O. Intracellular escape strategies of *Staphylococcus aureus* in persistent cutaneous infections. *Exp Dermatol.* 2020;30:1428-1439.
- Phillips T, Huitema L, Cepeda R, et al. Aberrant recruitment of leukocytes defines poor wound healing in patients with recessive dystrophic epidermolysis bullosa. *J Dermatol Sci.* 2020;100(3):209-216.
- Brandling-Bennett HA, Morel KD. Common wound colonizers in patients with epidermolysis bullosa. *Pediatr Dermatol.* 2010;27(1):25-28.
- Al Kindi A, Alkahtani AM, Nalubega M, et al. *Staphylococcus aureus* internalized by skin keratinocytes evade antibiotic killing. *Front Microbiol.* 2019;10:2242.
- Schnaith A, Kashkar H, Leggio SA, Addicks K, Kronke M, Krut O. *Staphylococcus aureus* subvert autophagy for induction of caspase-independent host cell death. *J Biol Chem.* 2007;282(4):2695-2706.
- Lawrence PK, Rokbi B, Arnaud-Barbe N, et al. CD4 T cell antigens from *Staphylococcus aureus* Newman strain identified following immunization with heat-killed bacteria. *Clin Vaccine Immunol.* 2012;19(4):477-489.
- Spaulding AR, Salgado-Pabon W, Kohler PL, Horswill AR, Leung DY, Schlievert PM. Staphylococcal and streptococcal superantigen exotoxins. *Clin Microbiol Rev.* 2013;26(3):422-447.
- Uebele J, Habenicht K, Ticha O, Bekeredian-Ding I. *Staphylococcus aureus* protein a induces human regulatory T cells through interaction with antigen-presenting cells. *Front Immunol.* 2020;11:581713.
- Wherry EJ, Kurachi M. Molecular and cellular insights into T cell exhaustion. *Nat Rev Immunol.* 2015;15(8):486-499.
- Ziegler C, Goldmann O, Hobeika E, Geffers R, Peters G, Medina E. The dynamics of T cells during persistent *Staphylococcus aureus* infection: from antigen-reactivity to in vivo anergy. *EMBO Mol Med.* 2011;3(11):652-666.
- Nystrom A, Bornert O, Kuhl T, et al. Impaired lymphoid extracellular matrix impedes antibacterial immunity in epidermolysis bullosa. *Proc Natl Acad Sci USA.* 2018;115(4):E705-E714.
- Alexeev V, Salas-Alanis JC, Palisson F, et al. Pro-inflammatory chemokines and cytokines dominate the blister fluid molecular signature in patients with epidermolysis bullosa and affect leukocyte and stem cell migration. *J Invest Dermatol.* 2017;137(11):2298-2308.
- Kaech SM, Cui W. Transcriptional control of effector and memory CD8+ T cell differentiation. *Nat Rev Immunol.* 2012;12(11):749-761.
- van Kessel KP, Bestebroer J, van Strijp JA. Neutrophil-mediated phagocytosis of *Staphylococcus aureus*. *Front Immunol.* 2014;5:467.
- Wagner C, Kotsougiani D, Pioch M, Prior B, Wentzensen A, Hansch GM. T lymphocytes in acute bacterial infection: increased prevalence of CD11b(+) cells in the peripheral blood and recruitment to the infected site. *Immunology.* 2008;125(4):503-509.
- Schroder K, Sweet MJ, Hume DA. Signal integration between IFN γ and TLR signalling pathways in macrophages. *Immunobiology.* 2006;211(6-8):511-524.
- Jamwal SV, Mehrotra P, Singh A, Siddiqui Z, Basu A, Rao KV. Mycobacterial escape from macrophage phagosomes to the cytoplasm represents an alternate adaptation mechanism. *Sci Rep.* 2016;6:23089.
- Mitchell G, Chen C, Portnoy DA. Strategies used by bacteria to grow in macrophages. *Microbiol Spectr.* 2016;4(3). Online ahead of print.
- Huang J, Brumell JH. Bacteria-autophagy interplay: a battle for survival. *Nat Rev Microbiol.* 2014;12(2):101-114.
- Kaufmann SH. Role of T-cell subsets in bacterial infections. *Curr Opin Immunol.* 1991;3(4):465-470.
- Kullander J, Forslund O, Dillner J. *Staphylococcus aureus* and squamous cell carcinoma of the skin. *Cancer Epidemiol Biomarkers Prev.* 2009;18(2):472-478.
- Madhusudhan N, Pausan MR, Halwachs B, et al. Molecular profiling of keratinocyte skin tumors links *Staphylococcus aureus* overabundance and increased human beta-Defensin-2 expression to growth promotion of squamous cell carcinoma. *Cancers (Basel).* 2020;12(3):541.
- Wood DLA, Lachner N, Tan JM, et al. A natural history of actinic keratosis and cutaneous squamous cell carcinoma microbiomes. *mBio.* 2018;9(5):e01432-18.
- Faedo RR, da Silva G, da Silva RM, et al. Sphingolipids signature in plasma and tissue as diagnostic and prognostic tools in oral squamous cell carcinoma. *Biochim Biophys Acta Mol Cell Biol Lipids.* 2022;1867(1):159057.
- Eierhoff T, Bastian B, Thuenauer R, et al. A lipid zipper triggers bacterial invasion. *Proc Natl Acad Sci USA.* 2014;111(35):12895-12900.

29. Xu SX, McCormick JK. Staphylococcal superantigens in colonization and disease. *Front Cell Infect Microbiol.* 2012;2:52.
30. Penalzoza-MacMaster P, Kamphorst AO, Wieland A, et al. Interplay between regulatory T cells and PD-1 in modulating T cell exhaustion and viral control during chronic LCMV infection. *J Exp Med.* 2014;211(9):1905-1918.
31. Park HJ, Park JS, Jeong YH, et al. PD-1 upregulated on regulatory T cells during chronic virus infection enhances the suppression of CD8+ T cell immune response via the interaction with PD-L1 expressed on CD8+ T cells. *J Immunol.* 2015;194(12):5801-5811.
32. Coden ME, Berdnikovs S. Eosinophils in wound healing and epithelial remodeling: is coagulation a missing link? *J Leukoc Biol.* 2020;108(1):93-103.
33. Wang R, Huang K. CCL11 increases the proportion of CD4+CD25+Foxp3+ Treg cells and the production of IL2 and TGFbeta by CD4+ T cells via the STAT5 signaling pathway. *Mol Med Rep.* 2020;21(6):2522-2532.

SUPPORTING INFORMATION

Additional supporting information may be found in the online version of the article at the publisher's website.

FIGURE S1 Analysis of RDEB keratinocyte infectivity with *Staphylococcus aureus* (red) in tricolour (RGB) image (panels to the left) as shown in Figure 1d and red channel only (panels to the right)

FIGURE S2 Analyses of the infectivity and intracellular trafficking of the *Staphylococcus aureus* in control and RDEB keratinocytes in tricolour (RGB) image as shown in Figure 2 and in split, red, green and blue channels as indicated

FIGURE S3 Indirect immunofluorescence analysis of PD-L1 (green) expression in *Staphylococcus aureus* (red)-infected and non-infected RDEB keratinocytes in tricolour (RGB) image, as shown in Figure 5e and in split red and green channels as indicated

Supplementary Material S1

TABLE S1 PCR primers for detection of microbial infection

TABLE S2 List of antibodies used in the study

TABLE S3 Wound dressing information

TABLE S4 Cells used in the study

How to cite this article: Alexeev V, Huitema L, Phillips T, et al.. T-cell activation and bacterial infection in skin wounds of recessive dystrophic epidermolysis bullosa patients. *Exp Dermatol.* 2022;31:1431-1442. doi: [10.1111/exd.14615](https://doi.org/10.1111/exd.14615)